Supplement of Atmos. Meas. Tech., 16, 2655–2672, 2023
https://doi.org/10.5194/amt-16-2655-2023-supplement

Atmospheric Measurement Techniques
Open Access
EGU

Supplement of

Characterizing the automatic radon flux transfer standard system Autoflux: laboratory calibration and field experiments

Claudia Grossi et al.

Correspondence to: Claudia Grossi (claudia.grossi@upc.edu)

Here we present the support material of the Grossi et al., manuscript: 'Characterizing the automatic radon flux Transfer Standard system *Autoflux*: laboratory calibration and field experiments'.

Table S1. Summary of the exhalation bed facilities studied.

Institution	F (mBq m^{-2} s^{-1})	Reference
CANMET Elliot lake Laboratory (Canada)	285 ± 41	Stieff et al. (1996)
Radon Laboratory of the University of South China	1480 ± 50	Tan & Xiao (2011)
Oak Ridge Associated Universities (USA)	430 to 80	Altic (2014)
Institute of Industrial Ecology (Russia)	700 ± 80	Onishchenko et al. (2015)
University of Huelva (Spain)	13.3 ± 0.2 23.4 ± 0.3	Gutiérrez-Álvarez et al. (2020)

Table S2. Sensor features used to monitor the environmental conditions.

Sensor	Manufacturer	Model	Range	Declared Accuracy
Temperature	Testo	175T2	(-35 to 55) ºC	±0.5 ºC
		Probe	(-40 to 120) ºC	±0.3 ºC
Soil moisture	ODYSSEY	Xtreem	(0 to 100) %	±1%
Pressure	ITEFI-CSIC	-	(-600 to 600) Pa	± 3 Pa

Figure S1. Picture of the setup used to empirically determine the exhalation rate reference value of the EB.

Table S3. Main characteristics of radon flux systems available from the literature.

Code	Manufacturer	Volume (m^3)	Exhalatio area (m^2)	Refresh*	Chamber shape	Radon monitor /mode	Environmental sensors within the monitor	Environ. Sensors within the Chamber	Source
1	ANSTO	0.019	0.13	Y	Drum	AG/Pump	Y	N	-
2	ANSTO	0.018	0.26	N	Shallow conical	AG2 x 1L lucas cells (separated by 6 min flow path)/Pump	Y	N	Zahorowski and Whittlestone, 1996
3	LICOR	0.041	0.03	Y	Hemisphere	-/Pump	-	N	https://www.licor.com/env/products/soil_flux/#chamber-difference
4	IPSN	0.037	0.21	Y	Cylinder	AG/Pump	Y	N	Ferry et al., 2001
5	Univ. of Wisconsin-Madiso	0.002, 0.018, 0.352	0.02 , 0.07, 2.32	N	Circular , Circular , Square	RAD7/Pump	Y	N	Stefani et al., 2016
6	Helmholtz Zentrum München	0.044	0.13	Y	Cylinder	6 Lucas cells/Pump	N	Y	Yang et al., 2017
7	UPC	-	0.01	Only pump	Cylinder	DOSEman/Diffusion	N	N	-
8	UC	0.008	0.04	Only pump	Rectangular	AlphE/Diffusion	N	N	-

1

2

3

4

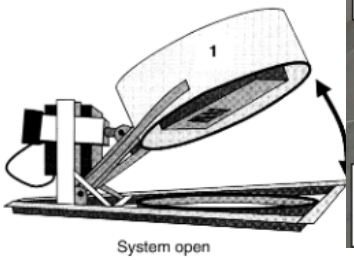

5

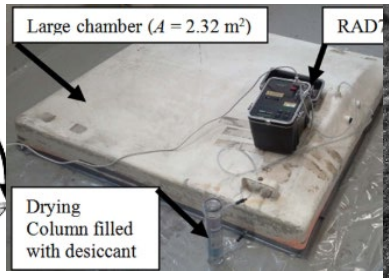

6

7

8

Figure S2. Pictures of enlisted radon chambers, code numbers correspond to those in Table S3.

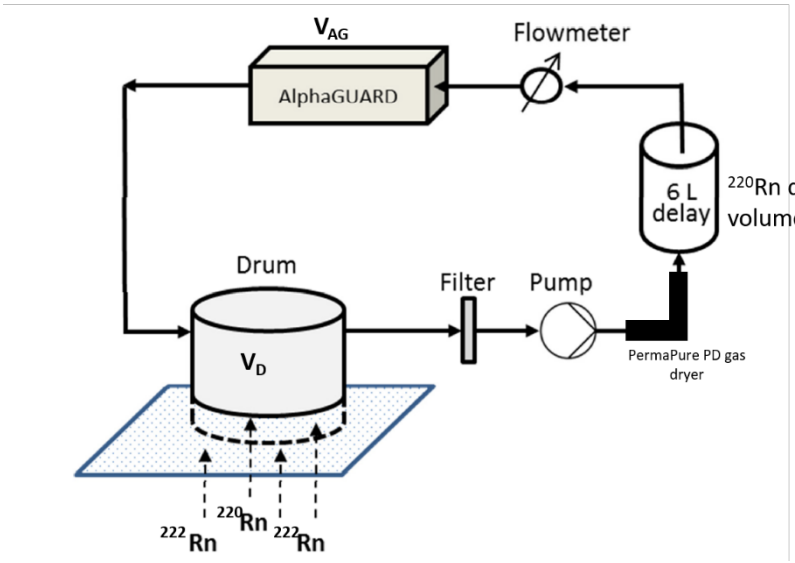

Figure S3. Schematic representation of the *AutoFlux* system (ANSTO).

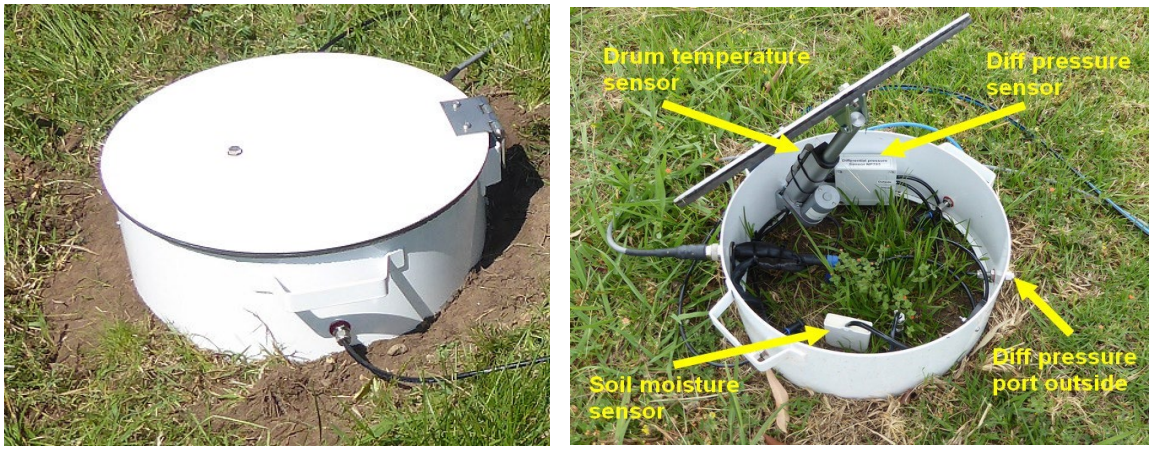

Figure S4. *AutoFlux* drum during a typical radon flux measurement: accumulation period (1 hour, on the left side) and ventilation period (2 hours, right side).

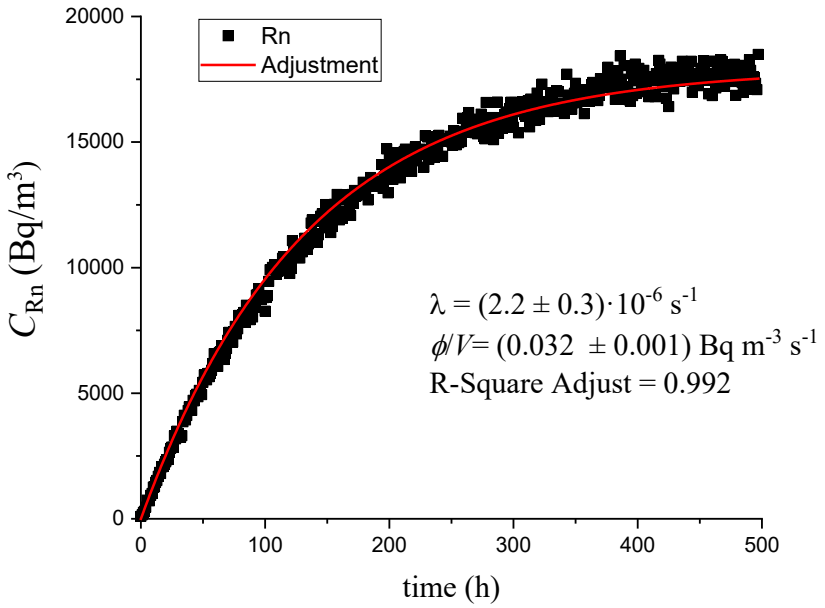

Figure S5. Evolution of radon concentration with time in a volume *V* during the experiment to establish the emanation factor *ε* of the radon from the soil sample. The coefficients of the exponential fit are presented.

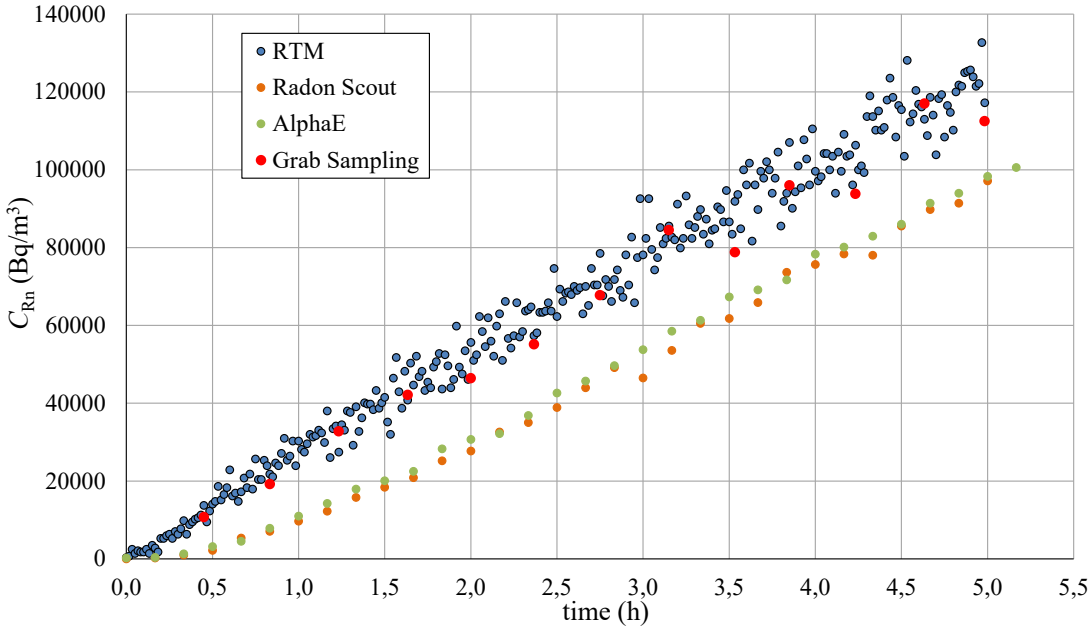

Figure S6. Example of radon concentration over time during the experimental determination of exhalation rate.

Figure S7. Setup of the *AutoFlux* during a typical laboratory measurement at UC.

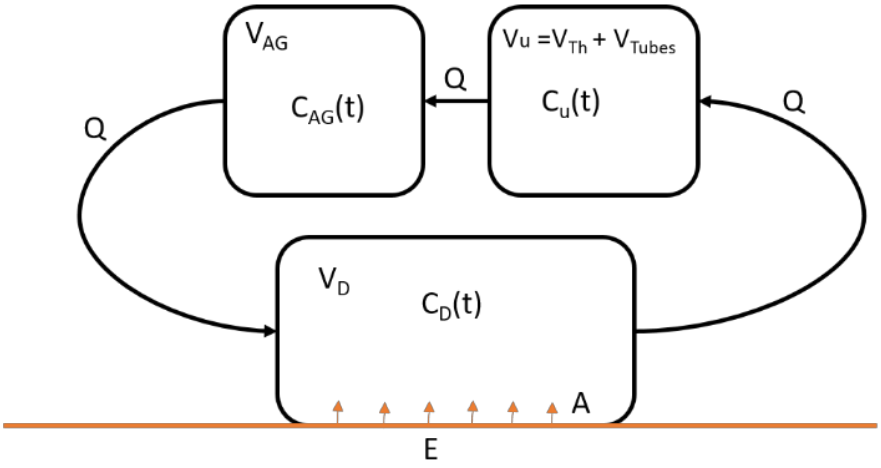

Figure S8. Conceptual box model of the ANSTO *AutoFlux* system.

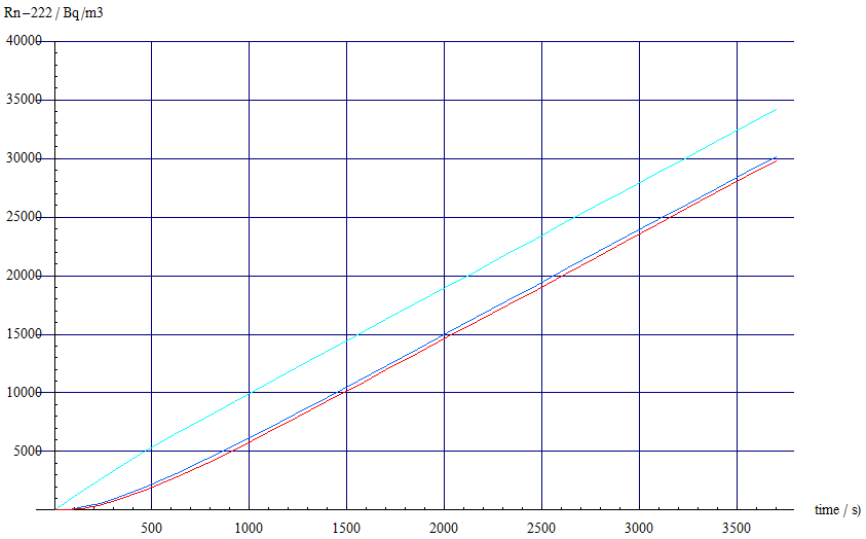

Figure S9. Simulated ^{222}Rn concentration behavior within each one of the volumes of the *AutoFlux* system during the hour for which the chamber was closed C_D (light blue line), C_u (blue line) and C_{AG} (red line).